Journal of Structural Geology, Vol. 9, No. 1, pp. 31 to 40, 1987
Printed in Great Britain

0191-8141/87 $03.00+0.00

Strain and deformation mechanisms in the Variscan nappes of Vendée, South Brittany, France

ALAIN VAUCHEZ, DANIEL MAILLET and JEAN SOUGY

Laboratoire de Géologie Dynamique and C.N.R.S. U.A. No. 132, Faculté des Sciences et Techniques St-Jérôme, 13397 Marseille Cedex 13, France

(*Received* 14 *May* 1985; *accepted in revised form* 28 *March* 1986)

Abstract—The Variscan nappes of Vendée (South Brittany, France) were displaced westward through a mechanism of regional subhorizontal ductile shear involving the entire body of the nappes. Ductile shear also affected the upper part of the Silurian footwall, including the rhyolite of Chapelle–Hermier, which was mylonitized and sheared with upward-increasing intensity, as well as the calcalkaline Vendée porphyroids of volcanic and volcanoclastic origin which form a mylonite sheet outlining the major basal thrust zone of the nappes. Nappe displacement was accompanied by a severe extensional strain, estimated at up to 300–400% in both the porphyroids and the rhyolite, and indicating that the deformational history may have involved a gravitational spreading component. Within the mylonitic rhyolite, accommodation of the bulk strain was mainly by solution-assisted mass-transfer, as shown by (1) growth of quartz fibres in low-pressure zones, (2) development of polycrystalline ribbons through continuous growth of quartz grains in pressure shadows and (3) crystallization of muscovite at the expense of the felsitic groundmass. A similar deformation process was probably active in the mylonitic porphyroids at the sole of the nappe, suggesting that pressure-solution flow was an important mechanism in nappe displacement.

INTRODUCTION

THE DEFORMATIONAL history of the Armorican Variscan belt is marked by early large-scale thrust tectonics (Cogné 1974, Lagarde 1978, Quinquis *et al.* 1978, Marchand 1981, Brun & Burg 1982) relating to the continent–continent collision following plate convergence (Bard *et al.* 1980). According to Autran (1978) and Brun & Burg (1982), thrusting occurred before Upper Devonian strata were deposited on folded rocks of Silurian and Lower Devonian age (Ters 1979). This timing is consistent with Rb–Sr whole rock ages of *c.* 370 Ma obtained by Vidal (1980) on various anatectic granites that post-date nappe motion.

The analysis of these early structures is often difficult because they are overprinted by Carboniferous ductile strike-slip features responsible for the most obvious structural patterns (Jegouzo 1980). South-west of the 'South Armorican Shear Zone' (S.A.S.Z., see Fig. 2), however, transcurrent movements are of only moderate intensity and, as a result, the early structures are retained (Burg 1981). For this reason the coastal Vendée is of particular interest for a study of nappe-related structures.

This paper presents the results of a detailed analysis of the basal thrust zone and the rocks immediately below and above, in an attempt to elucidate the mechanism of the strain that gave rise to the displacement of the nappes.

THE VENDEE NAPPES

The structure of the Variscan orogen in the coastal Vendée (Figs. 1 and 2) consists mainly of a stack of subhorizontal nappes which have been displaced westward across a strongly deformed subautochthonous Siluro-Ordovician footwall (Burg 1981, Brun & Burg 1982, Maillet 1984).

The nappes

From bottom to top (Fig. 1), the nappe pile is composed of the following units (Burg 1981).

(1) A calcalkaline volcanic and volcanoclastic formation (Vendée porphyroids), which has been strongly mylonitized and metamorphosed to greenschist facies (Fig. 2).

(2) A thick sequence of feldspathic schists (St. Gilles schists) containing muscovite and locally biotite and garnet.

(3) A unit of glaucophane schists associated with serpentine (Bois de Céné blueschists). Together with

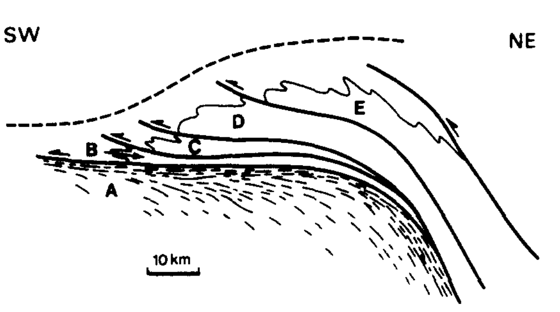

Fig. 1. Hypothetical sketch section of the Vendée region showing an orogenic welt produced by piling up of the Variscan allochthonous units after they were pushed away from a suture zone by continental collision: A, Siluro–Ordovician basement; B, porphyroids and St. Gilles schist unit; C, HP/LT blueschist unit; D, leptyno-amphibolitic (oceanic crust) unit; E, Precambrian and Lower Palaeozoic exotic terranes.

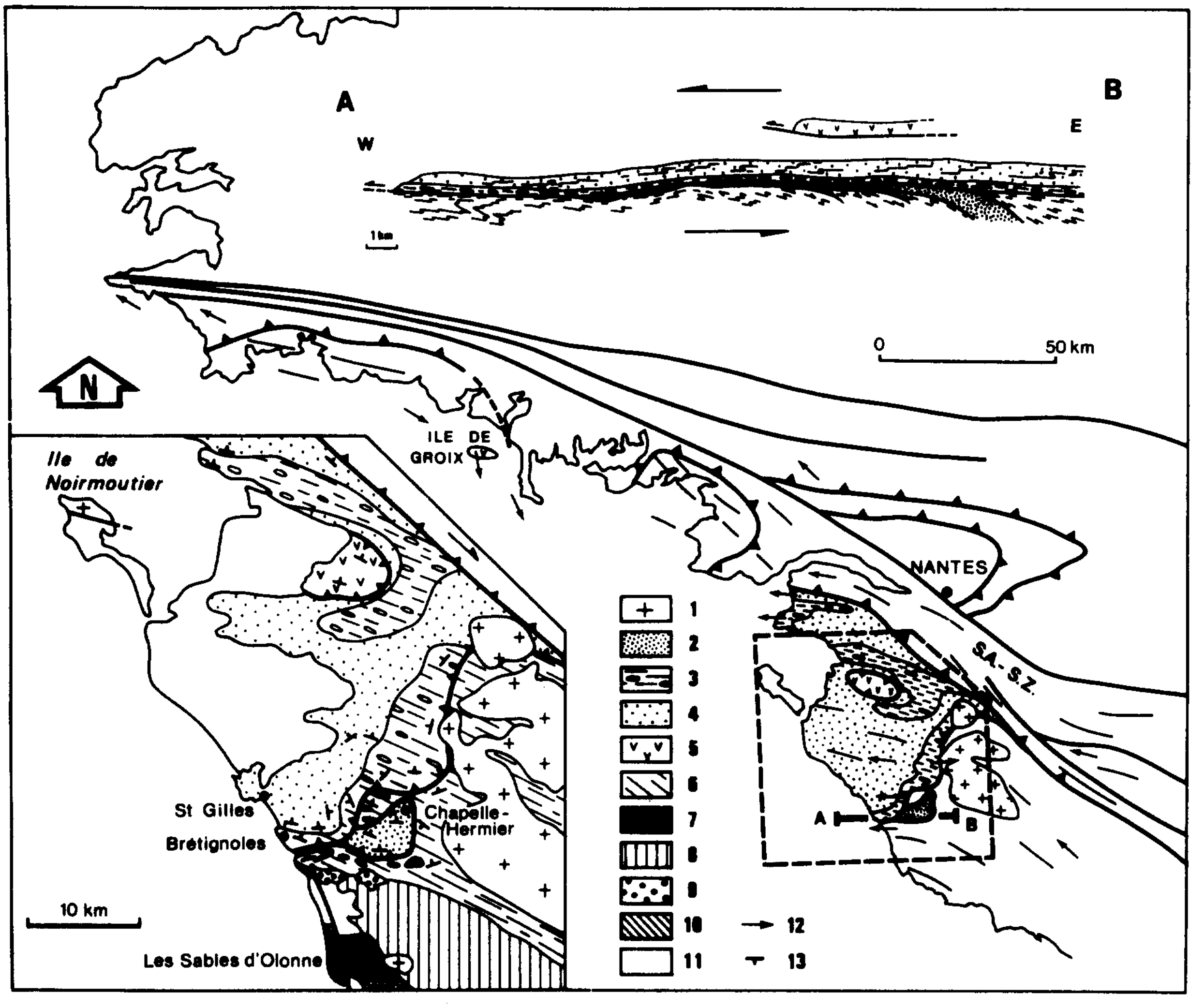

Fig. 2. Regional map to show thrusting in the South Armorican Hercynian belt (modified from Brun & Burg 1982). Inset geological sketch map (modified from Ters 1980) and cross-section of the southern part of the nappe pile of Vendée. The schematic cross-section shows the configuration at the end of the westward motion of the nappes; subsequent tectonic and magmatic events have been removed. (1) Granite, (2) Chapelle–Hermier metarhyolite, (3) Vendée porphyroids, (4) feldspathic schists of St. Gilles, (5) blueschists of Bois de Céné, (6) Silurian metasediments, (7) siliceous shales, (8) Ordovician, (9) rhyolite, (10) metamorphic complex of Les Sables d'Olonne, (11) Mesozoic to Quaternary terranes, (12) stretching lineation, (13) foliation. S.A.S.Z. = South Armorican Shear Zone.

the Île de Groix blueschists this unit forms a HP/LT metamorphic belt which probably resulted from the subduction of an oceanic floor prior to continental collision (Boudier & Nicolas 1976, Carpenter & Civetta 1976, Quinquis & Choukroune 1981).

(4) A leptyno-amphibolitic unit showing chemical characters of an oceanic crust (Montigny & Allègre 1974), transected to the north by the S.A.S.Z.

The footwall

The footwall below the nappes consists of a sequence of alternating metapelites and metasandstones with some calcareous beds. Abundant microfossils at the top of the sequence reveal a Silurian age (Ters 1970). The upper part of the sequence is marked by (i) both siliceous and carbonaceous shales and (ii) extrusive rocks of mostly rhyolitic composition (Chapelle–Hermier rhyolite) resulting from a calcalkaline volcanic event of regional extent. This rhyolitic massif was previously recognized as deformed and metamorphosed during the Variscan orogeny (Ters 1977); it is overlain by the Vendée porphyroids.

TOP OF THE FOOTWALL

Iglesias & Brun (1976) pointed out strain anomalies in the Silurian terranes along the coast south of Brétignoles (Fig. 2), near the contact with the porphyroids. We have carried out a more detailed study of the rocks just below the basal thrust of the nappe pile in the same area, where the Silurian metasediments are well exposed and the evolution of the deformation can be studied, as well as farther inland where the Silurian Chapelle–Hermier rhyolite exhibits a strong upward deformation gradient.

Deformation of Chapelle–Hermier rhyolite

Toward the allochthonous units, the Chapelle–Hermier rhyolite is increasingly deformed and exhibits a

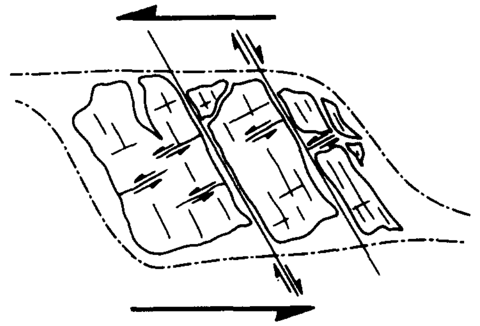

Fig. 3. Sketch of rotation-induced fractures in feldspar.

mylonitic fabric consisting of a fluxion structure (Tullis *et al.* 1982) and grain-size reduction caused by both fracturing of feldspar phenocrysts and dynamic recrystallization of quartz (less commonly of feldspar) phenocrysts.

The most prominent feature evident from strain analysis is that the extensional component of strain is dominant. Many observations support this statement.

(1) Feldspar megacrysts initially parallel to the foliation plane show the effects of large finite extensions. Intense stretching was accommodated both by fracturing at right angles to the extension axis, and by pulling apart of the fragments. The offset between two fragments is frequently large compared with the initial length of the crystal, and the displacement is parallel to the stretching lineation.

(2) Fibrous quartz has crystallized within the gaps opened in phenocrysts (and less commonly within shadow zones around phenocrysts) and has subsequently suffered dynamic recrystallization. Fibres commonly are a few mm long parallel to the stretching lineation. This pattern is similar to crack–seal deformation described by Ramsay (1980b) and Cox & Etheridge (1983) and is discussed in more detail in a later section.

(3) There is a prominent E–W stretching lineation.

(4) We have computed the magnitude of extensional strain $(1 + e_1)$, using Ferguson's method (Ferguson 1981, Ferguson & Lloyd 1984). The maximum values range commonly between 2.5 and 3.

Many observations at various scales suggest a progressive non-coaxial deformation resulting from westward subhorizontal shearing. These include the following.

(1) Asymmetry of pressure-shadows and recrystallized tails exhibited around most phenocrysts.

(2) Intracrystalline fracturing of feldspar phenocrysts initially oblique to the foliation, but reoriented with increasing strain by rotation within the more ductile matrix (Fig. 3). This rigid body rotation has frequently induced antithetic intracrystalline fractures along which fragments have slipped oblique to the foliation. The orientation of fractures indicates a constant sense of rotation of phenocrysts consistent with non-coaxial strain.

(3) An asymmetrical pattern of preferred orientation of quartz *c*-axes (Fig. 4).

(4) The development, in moderately deformed areas, of flat-lying shear zones ranging in thickness from 10's of cm to 10's of metres (e.g. in the quarry of La Chilloue).

Deformation of the Silurian metasediments

Approaching the thrust zone, the structural evolution is characterized by:

(1) An increasingly prominent E–W stretching lineation within the S_1-foliation. Close to the contact, in shales containing cm- to dm-scale quartzitic layers of greater competence, this evolution results in the disruption of the bedding and in the occurrence of a linear mylonitic fabric.

(2) Rotation of the hinges of folds contemporaneous with ductile thrusting, in contrast to the constant E–W direction of the stretching lineation. These folds, most of

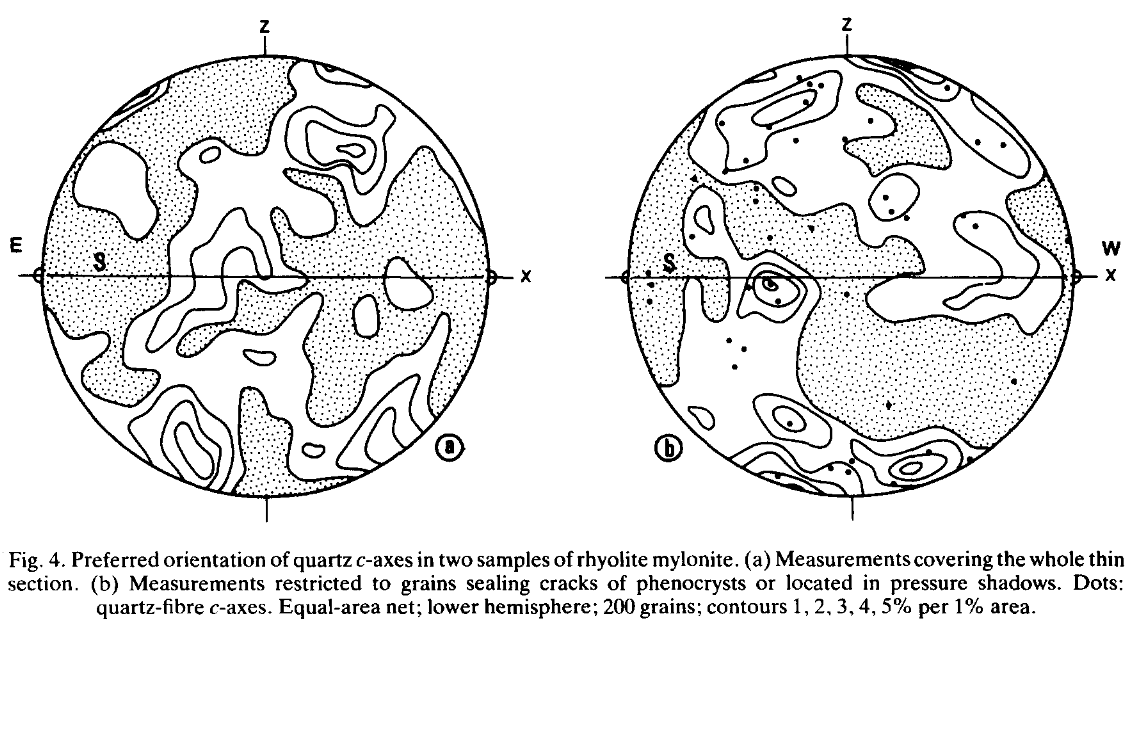

Fig. 4. Preferred orientation of quartz *c*-axes in two samples of rhyolite mylonite. (a) Measurements covering the whole thin section. (b) Measurements restricted to grains sealing cracks of phenocrysts or located in pressure shadows. Dots: quartz-fibre *c*-axes. Equal-area net; lower hemisphere; 200 grains; contours 1, 2, 3, 4, 5% per 1% area.

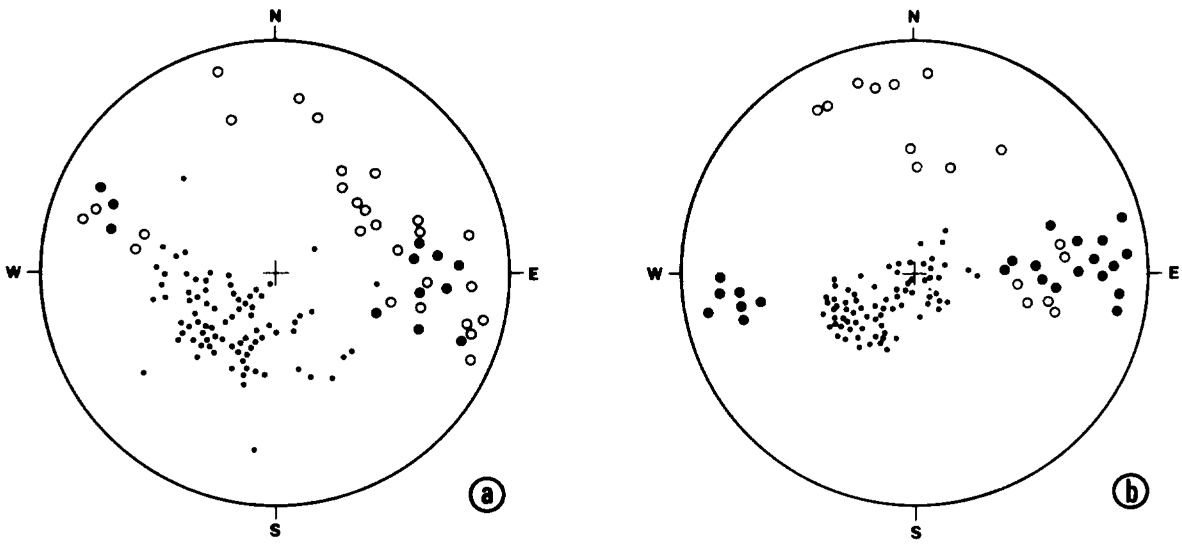

Fig. 5. Equal-area lower hemisphere projections showing rotation of the axial trends of contemporary folds within the mylonite foliation plane. (a) Porphyroids, north of Brétignoles. (b) Silurian basement, some tens of metres below the porphyroids. Open circles: fold axes; filled circles: stretching lineation; dots: poles of foliation planes.

them isoclinal, are overturned or recumbent: their axes are scattered within the mean plane of the mylonitic foliation (Fig. 5a). This pattern may be related to the development of non-cylindrical folds during progressive non-coaxial deformation (Williams 1978, Berthé & Brun 1980).

(3) An increase in the number of sheath folds (Cobbold & Quinquis 1980) independent of lithological variations. These have a trend parallel to the E–W stretching lineation and are synchronous with the S_1-foliation.

(4) A reorientation of more competent beds (m-scale layers of siliceous shale).

These suggest that the Silurian footwall was sheared during nappe displacement and experienced a large finite strain.

DEFORMATION WITHIN THE PORPHYROID SHEET

The base of the allochthonous pile is systematically outlined by the Vendée porphyroids, a unit which forms a sheet less than 100 m thick. These rocks typically contain feldspar and quartz phenocrysts, generally strongly deformed, but there are a few still with their original crystal shapes. The phenocrysts are surrounded by a matrix showing alternating muscovite-rich and quartz-rich layers, the latter with a strong lattice-preferred orientation (Burg 1981), and some relics of a fine-grained groundmass preserved, in most cases, in phenocryst embayments. The flat-lying mylonitic foliation contains a strong stretching lineation, marked (Fig. 7) by elongated or fractured phenocrysts, banded recrystallized quartz, and preferred orientation of phyllosilicates. Those are accompanied by a feldspar lineation in coarse-grained facies and a corrugation lineation in finer ones. The different types of lineation have a systematic E–W trend.

The analysis of deformation features in these mylonites suggests:

(1) *A subhorizontal shear to the west*, as indicated by (i) asymmetrical pressure-shadows and recrystallized tails; (ii) intracrystalline fracturing related to rotation of feldspar phenocrysts, always in the same sense; (iii) an asymmetrical distribution of quartz *c*-axes (Burg 1981); (iv) 'S–C' planar fabric (Berthé *et al.* 1979, Simpson & Schmid 1983), observed at both macroscopic and microscopic scales, but most common in thin section; (v) retort-shaped crystals (Etchecopar 1977, Simpson 1983) resulting from shear strain gradients at the grain scale: part of the crystal remained undeformed because of a lattice orientation unfavourable to slip; the remainder was reoriented by lattice rotation thus facilitating slip, and was strongly sheared and stretched into a shear band; and (vi) a scattering of the trends of contemporary fold axes in the mean S_1-foliation surface, contrasting with a constant stretching lineation close to E–W (Fig. 5b).

(2) *A dominant extensional component of strain*, as shown by (i) a prominent stretching lineation, frequently accompanied by corrugation in the same direction, a feature commonly related to large elongation of the material (Burg 1981); (ii) feldspar phenocrysts fracturing perpendicular to the stretching lineation and the pulling apart of the fragments; (iii) extensive crystallization of fibrous quartz; (iv) values of maximum finite stretch $(1 + e_1)$ computed using Ferguson's method ranging commonly between 1.1 and 4.7; and (v) according to Burg (1981), quartz *c*-axes lying preferentially in a small circle distribution around the stretching lineation, a pattern commonly correlated with extensional strain (Lister & Hobbs 1980).

In summary, field and microscope studies of the footwall close to the basal thrust zone, as well as of the bottom of the nappe pile, clearly show that strain is characterized by (1) westward directed shear, and (2) a large extensional component of strain.

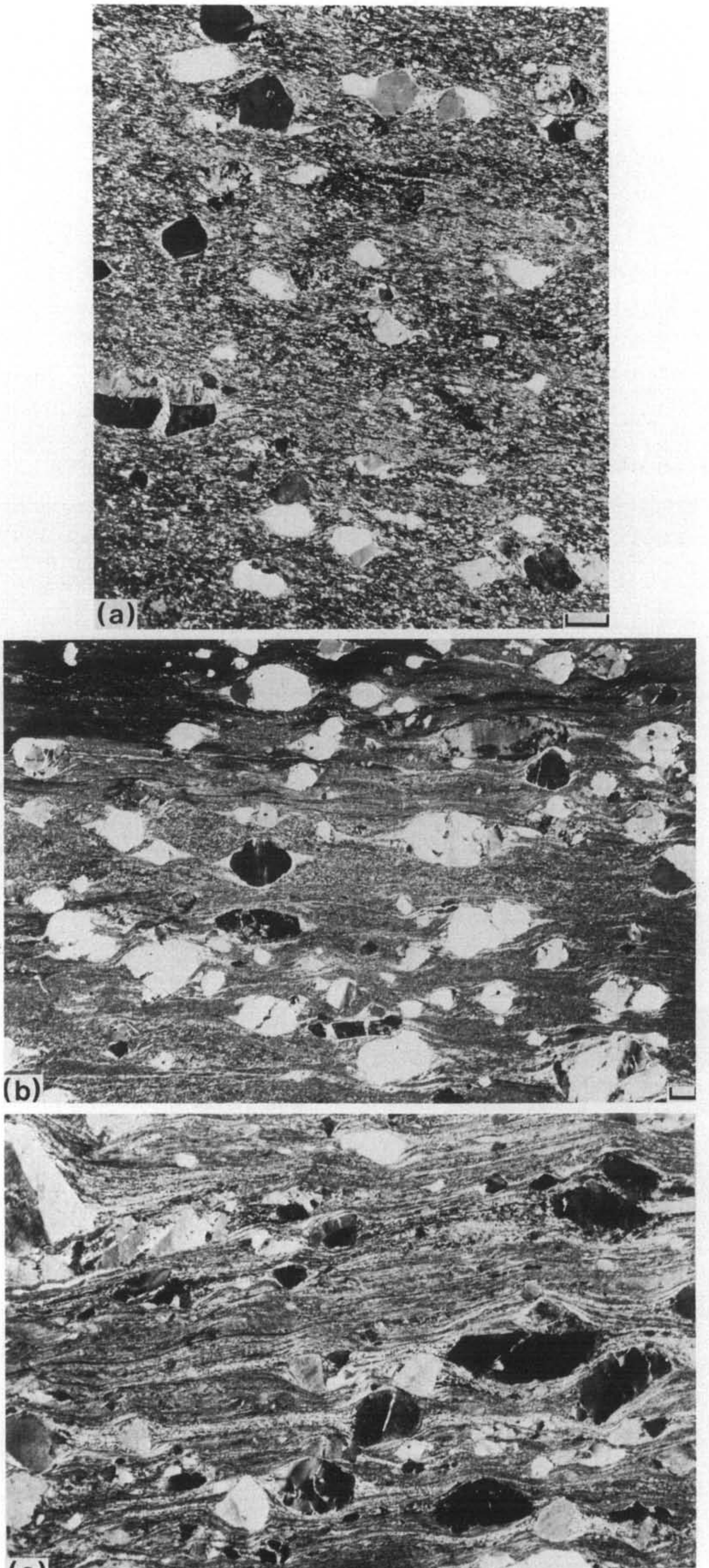

Fig. 6. Three samples of mylonitized Chapelle–Hermier rhyolite, with deformation increasing from (a) to (c) showing: the development of a mylonitic foliation with quartz ribbons; the decreasing volume of groundmass and the fracturing of feldspar phenocrysts. Crossed nicols. Scale bar is 1 mm.

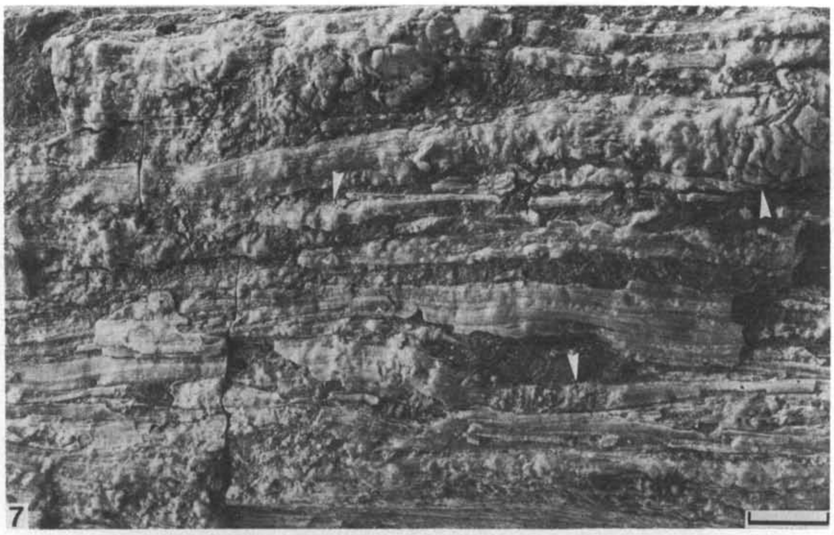

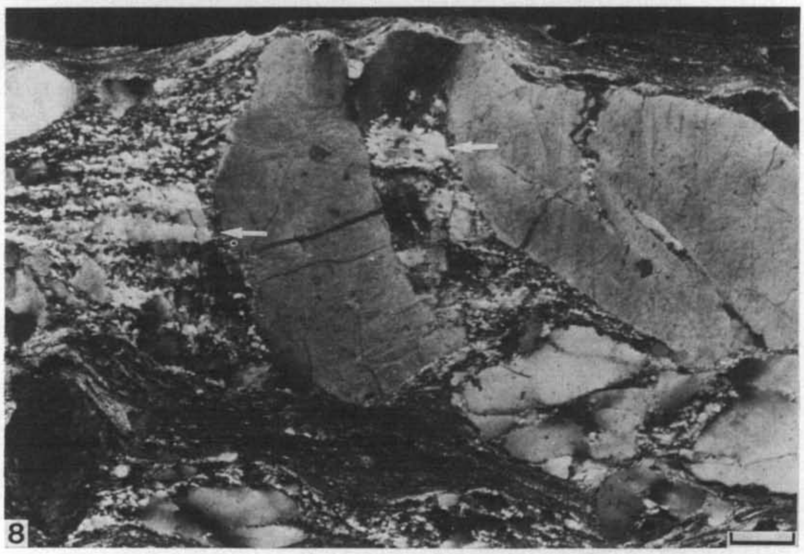

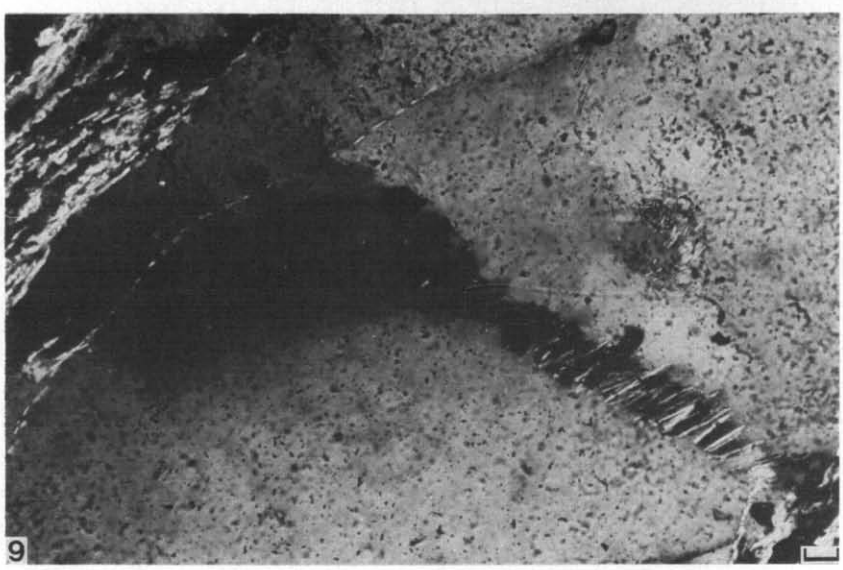

Fig. 7. Foliation in the Vendée porphyroids. Lineation is characterized by banded quartz and fractured feldspar phenocrysts (arrows). Scale bar is 1 cm.

Fig. 8. Photograph of a fractured feldspar crystal showing fibrous quartz crystallized in the gap between two fragments and in the pressure shadow (arrows). Crossed nicols. Scale is 0.5 mm.

Fig. 9. Small needles of sericite crystallized along a zone of dynamic recrystallization within quartz phenocrysts and parallel with those in the foliation around the phenocryst. Crossed nicols. Scale is 10 μm.

The production of very large extensional strains during shearing in a subhorizontal thrust zone may be related to gravitational spreading of the Vendée nappes during their deformational history. Regarding gravitational spreading, Hudleston (1977) writes "for gravitational flow to occur it is not necessary for the basement or rigid substrate surface to dip in the direction of shear displacement, but it is necessary for the upper surface of the cover material to slope in that direction". According to Elliott (1976) and Hudleston (1977) such a process may have occurred in orogenic zones where an orogenic welt, formed as a result of the stacking of allochthonous sheets, gave rise to gravitational flow. These geometrical conditions would have been satisfied during the Variscan continental collision following plate convergence, when allochthonous sheets were pushed forward from a suture zone and piled up on a continental plate, where they underwent large subhorizontal displacements (Fig. 1).

MYLONITIZATION AND DEFORMATION MECHANISMS IN THE SOLE OF THE NAPPE PILE

The successive stages of mylonitization preserved in the Chapelle–Hermier metarhyolite provide a good opportunity for a study of deformation processes acting during nappe motion. The observations presented below were made on the metarhyolite, but they should hold for the porphyroid unit as well as because: (i) both originated from calcalkaline volcanic rocks of mainly rhyolitic composition (Ters 1977), and their initial textures were undoubtedly similar; (ii) they underwent the same deformational history; and (iii) their present mylonitic textures exhibit similar characteristics, suggesting comparable behaviour during deformation.

The original rock

The Chapelle–Hermier rhyolite, described by Ters (1977), is composed of a devitrified felsitic groundmass containing: (i) quartz and feldspar grains <5 μm in size; (ii) uncommon fine-grained sericite and (iii) a variable proportion of spherulites. There are a large proportion of subautomorphic quartz and feldspar phenocrysts. Both show embayments in which the devitrified groundmass has been preserved. Some of the feldpar is sanidine, but the greater part is microcline and orthoclase. Minor apatite, zircon and biotite also occur.

Deformation of quartz phenocrysts

In the less deformed samples (Fig. 6a) quartz grains are globular and free of substructures, and small pressure shadows have developed at their edges. With increasing strain phenocrysts become lens-shaped (Fig. 6b) and exhibit spaced prismatic sub-grain boundaries. More elongated quartz phenocrysts (shape-ratios $\leqslant 3:1$) show tight prismatic sub-grain boundaries, deformation bands, deformation lamellae that are commonly subbasal and less commonly subprismatic, and equidimensional sub-grains located along deformation bands, within zones of strong lattice bending and along grain boundaries. In still more deformed samples (Fig. 6c) dynamic recrystallization becomes important in quartz phenocrysts, producing strain-free equidimensional neoblasts (25–30 μm). These were initially located in the more strained portions of the crystals (deformation bands, zones of lattice bending, and grain boundaries). Moreover many quartz phenocrysts are truncated by muscovite-rich layers, suggesting stress-induced dissolution of faces parallel to the mylonitic layering.

This evolution of quartz microstructure during progressive deformation is typical of low temperature conditions (Tullis *et al.* 1973, Bouchez 1977), consistent with the activation of the basal $\langle a \rangle$ slip system suggested by the *c*-axis fabric (Fig. 4), as well as with the low degree of metamorphism recorded by the mylonites.

Deformation of feldspar phenocrysts

The behaviour of feldspar phenocrysts was mainly rigid–brittle. Many were probably fractured during the first increments of strain (Fig. 6a). As previously discussed, two cases of fracturing can be distinguished:

(1) rotation-induced fracturing when the crystal was oriented oblique to the foliation; and

(2) extensional fracturing and pulling apart of the fragments when crystals were parallel to the foliation.

In most mylonitized samples, feldspar phenocrysts display well defined deformation bands and kink-bands parallel to the foliation. Both sub-grains and new grains may occur along boundaries of deformation bands. This type of microstructure suggests an accommodation mechanism in which dislocation creep was more important and was accompanied by dynamic recovery and minor dynamic recrystallization (Tullis & Yund 1985). Many phenocrysts have a chessboard structure (Ters 1977) resulting from synkinematic perthitization (Spry 1968, Laurent 1974).

The origin of quartz ribbons

Quartz ribbons developed independently of the onset of dynamic recrystallization of quartz phenocrysts, as shown by the fact that they are well developed in samples in which dynamic recrystallization was inactive or incipient. The process which most reasonably accounts for the development of quartz ribbons is mass-transfer, probably solution-assisted, of silica from the groundmass into low-pressure zones favourable to crystal growth. Two cases may be distinguished (Fig. 10):

(1) Crack–seal deformation mechanism (Ramsay 1980a, Cox & Etheridge 1983) in feldspar phenocrysts. Extensional fractures are opened and the fragments pulled apart. Because the pressure is locally lowered between displaced fragments, the most diffusive phase of the felsitic groundmass (i.e. silica) migrates into the cracks by solution-assisted mass-transfer and quartz grains crystallize (Figs. 10a and 8). Repeated crack–seal

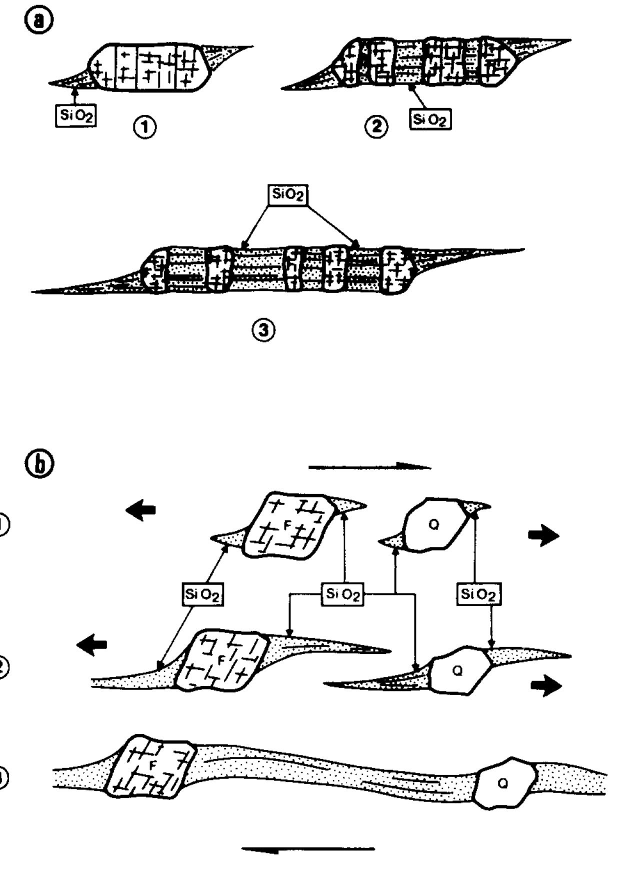

Fig. 10. Sketches showing two models for quartz ribbon development. The first (a) involves crack–seal deformation, that is extensional fracturing of feldspar, pulling-apart of the fragments and sealing of the gaps by newly crystallized quartz grains. The second (b) involves continuous growth of quartz grains in pressure shadows (1). This process results in the development of elongate crystalline tails (2) which anastomose and form ribbons (3). The symbol SiO_2 represents silica migrating from the groundmass to low-pressure zones.

increments led to the growth of fibres parallel to the extension axis. With increasing strain, these fibres may undergo dislocation creep and dynamic recrystallization.

(2) Growth and coalescence of elongate polycrystalline quartz aggregates resulting from continuous addition of quartz to pressure shadows (Figs. 10b and 8). This process involves repeated detachment of quartz aggregates from the phenocrysts and sealing by the growth of a new generation of quartz grains.

Deformation and evolution of the felsitic groundmass

With increasing mylonitization, the evolution of the felsitic groundmass is marked by the following features.

(1) A large decrease in its proportion in the mylonite, with an accompanying increase in the proportions of quartz ribbons and muscovite. In little deformed samples (e.g. Fig. 6a) the groundmass (including spherulites) forms between 60 and 70% of the rock, quartz and feldspar phenocrysts 15–30%, quartz aggregates in pressure shadows less than 10%, and muscovite and sericite less than 5%. In the most mylonitized samples (Fig. 6c), these proportions are 20–40% groundmass, 15–20% phenocrysts, 20–25% quartz ribbons and 20–30% muscovite-rich layers.

(2) A decrease in the ratio of spherulitic to non-spherulitic groundmass.

(3) Crystallization of sericite grains along fractures or recrystallized bands within phenocrysts (Fig. 9).

The development of a compositional layering during the mylonitization of the Chapelle–Hermier rhyolite probably results from a process similar to that of metamorphic segregation as defined by Robin (1979), which can lead to mylonitic banding. It involves (1) diffusion transfer of silica from the groundmass to low pressure zones where quartz grains are able to grow and (2) crystallization of a large amount of muscovite probably through a reaction such as: feldspar $\rightarrow$ muscovite + quartz (Beach 1976, Bossière 1980). This reaction requires hydration of the mylonite, that is diffusion of a hydrous solution through the rock, which is also indicated by crystallization of sericite within phenocrysts (Cox & Etheridge 1983). According to Robin (1979), the growth of a large number of muscovite flakes and the development of mica-rich layers may enhance pressure solution and the migration of silica from the groundmass to the quartz-rich domains.

Silica transfer would be restricted, at least in large part, to the interlayer scale. Low-pressure zones where silica may crystallize are initiated around or between large grains or clasts, which are regularly distributed in the groundmass (e.g. Fig. 6a); and it may be assumed that the quartz grains within ribbons have crystallized from silica migrating from neighbouring mica-rich or groundmass-rich layers. On the other hand, chemical analyses published by Ters (1977) and discussed by Maillet (1984) suggest that during mylonitization the rock system was chemically open. For increasing strain there is (1) an increase in the Al_2O_3 and K_2O content and (2) a decrease in the Na_2O content. Silica content seems to decrease with increasing strain, but the correlation is weak. It follows that limited migration at a scale larger than the scale of the sample may be assumed, and this may be an indicator of the volume change.

The extent to which intracrystalline plasticity within quartz ribbons has contributed to the bulk deformation is difficult to determine. Dynamic recrystallization of quartz fibres implies dislocation creep. Crystallographic preferred orientation of quartz ribbons also suggests crystalline plasticity. However, the *c*-axis pattern argues for a more complex origin. Quartz *c*-axes in both equidimensional grains and fibres, measured in pressure shadows and in the gaps between feldspar phenocrysts fragments, are presented in Fig. 4(b) and there is a good correlation between the concentration of *c*-axes and the crystallographic orientation of fibres. This may signify that a lattice-preferred orientation developed during grain growth following mass transfer (Cox & Etheridge 1983). On the other hand, the highest concentration of *c*-axes is located near the pole of the foliation, suggesting the activation of the basal $\langle a \rangle$ slip system (Nicolas & Vialon 1980). On the basis of the *c*-axis fabric pattern and the dynamic recrystallization of most of the fibres, it may be assumed that dislocation creep was an efficient deformation mechanism in neoblasts and fibres, and brought about an alteration of the crystallographic fabric resulting from synkinematic grain growth.

CONCLUSIONS

(1) Westward displacement of the Variscan nappes of the coastal Vendée, previously pointed out by Burg (1981) and Brun & Burg (1982), is corroborated. It resulted from major subhorizontal ductile shear involving the allochthonous units as well as the Silurian footwall, which is increasingly strained upon approaching the basal thrust of the nappes.

(2) Pressure solution was an important, and perhaps dominant, deformation mechanism accommodating nappe displacement. It led to the development of mylonitic banding in metavolcanics sheared in the basal thrust zone. Such a mechanism was previously considered by Etheridge & Vernon (1981) for deformation of metavolcanics, and by Elliott (1976) for nappes sliding along discrete surfaces. In the present case, the motion of the allochthonous units is not accommodated by slip on discrete surfaces but by a regional penetrative non-coaxial deformation in a zone of ductile shear.

(3) An unusually large extensional component of strain in the basal thrust zone indicates a possible mechanism of nappe motion, involving the development of a gravitational spreading component (Elliott 1976, Hudleston 1977) after the nappes were pushed forward from the suture zone.

Acknowledgements—We are very grateful to R. Scholten for a critical review and improvement of the English.

REFERENCES

Autran, A. 1978. Synthèse provisoire des éléments calédoniens en France. *Geol. Surv. Pap. Can.* **78–13**, 159–175.

Bard, J. P., Burg, J. P., Matte, P. & Ribeiro, A. 1980. La chaîne hercynienne d'Europe occidentale en termes de tectonique des plaques. *26th Int. geol. Congr. Paris Report C6*, 233–246.

Beach, A. 1976. The interrelations of fluid transport, deformation, geochemistry and heat flow in early Proterozoic shear zones in the Lewisian complex. *Phil. Trans. R. Soc.* **A280**, 569–604.

Berthé, D., Choukroune, P. & Jegouzo, P. 1979. Orthogneiss, mylonite and non-coaxial deformation of granites; the example of the South Armorican shear zone. *J. Struct. Geol.* **1**, 31–42.

Berthé, D. & Brun, J.-P. 1980. Evolution of folds during progressive shear in the South Armorican Shear Zone, France. *J. Struct. Geol.* **2**, 127–133.

Bossière, G. 1980. Un complexe métamorphique polycyclique et sa blastomylonitisation. Etude pétrologique de la partie occidentale du Massif de Grande Kabylie (Algérie). Thèse de Doctorat d'Etat, Université de Nantes.

Bouchez, J.-L. 1977. Le quartz et la cinématique des zones ductiles. Thèse de Doctorat d'Etat, Université de Nantes.

Boudier, F. & Nicolas, A. 1976. Interprétation nouvelle des relations entre tectonique et métamorphisme dans l'Ile de Groix (Bretagne). *Bull. Soc. geol. Fr.* **18**, 135–144.

Brun, J.-P. & Burg, J.-P. 1982. Combined thrusting and wrenching in the Ibero-armorican arc: a corner effect during continental collision. *Earth Planet. Sci. Lett.* **61**, 319–332.

Burg, J.-P. 1981. Tectonique tangentielle hercynienne en Vendée littorale. Signification des linéations d'étirement E–W dans les porphyroides à foliation horizontale. *C. r. Acad. Sci. Paris* **293, 2**, 849–854.

Carpenter, M. S. N. & Civetta, L. 1976. Hercynian high pressure–low temperature metamorphism in the Île de Groix blueschists. *Nature, Lond.* **262**, 276–277.

Cobbold, P. R. & Quinquis, H. 1980. Development of sheath folds in shear regimes. *J. Struct. Geol.* **2**, 119–126.

Cogné, J. 1974. Les grandes lignes structurales du Massif Armoricain. In: *Franz Kossmat symp., Nov. Act. Leopoldina* **224**, 177–184.

Cox, S. F. & Etheridge, M. A. 1983. Crack–seal fiber growth mechanisms and their significance in the development of oriented layer silicate microstructures. *Tectonophysics* **92**, 147–170.

Elliott, D. 1976. The energy balance and deformation mechanisms of thrust sheets. *Phil. Trans. R. Soc.* **A283**, 289–312.

Etchecopar, A. 1977. A plane kinematic model of progressive deformation in a polycrystalline aggregate. *Tectonophysics* **39**, 121–139.

Etheridge, M. A. & Vernon, R. H. 1981. A deformed polymictic conglomerate—The influence of grain size and composition on the mechanism and rate of deformation. *Tectonophysics* **79**, 237–254.

Ferguson, C. C. 1981. A strain reversal method for estimating extension from fragmented rigid inclusions. *Tectonophysics* **79**, T43–52.

Ferguson, C. C. & Lloyd, G. E. 1984. Extension analysis of stretched belemnites: a comparison of methods. *Tectonophysics* **101**, 199–206.

Hudleston, P. J. 1977. Similar folds, recumbent folds, and gravity tectonics in ice and rocks. *J. Geol.* **85**, 113–122.

Iglesias, M. & Brun, J.-P. 1976. Signification des variations et anomalies de la déformation dans un segment de la chaîne hercynienne (Les séries cristallophyliennes de la Vendée littorale, Massif armoricain). *Bull. Soc. géol. Fr. 7 Sér.* **18**, 1443–1452.

Jegouzo, P. 1980. The South Armorican Shear Zone. *J. Struct. Geol.* **2**, 39–47.

Lagarde, J. L. 1978. La déformation des roches dans les domaines à schistosité subhorizontale. Application à la nappe du Canigou-Roc de France (Pyrénées orientales) et au complexe cristallophyllien de Champtoceaux (Massif Armoricain). Thèse 3e cycle Université de Rennes.

Laurent, P. 1974. Structure et pétrologie de la bande blastomylonitique de Badajoz-Cordoba (chaîne hercynienne sud-ibérique) à l'Est d'Azuaga (Espagne). Description et interprétation de la déformation dans les blastomylonites. Thèse 3e cycle Université de Montpellier.

Lister, G. S. & Hobbs, B. E. 1980. The simulation of fabric development during plastic deformation and its application to quartzite: the influence of deformation history. *J. Struct. Geol.* **2**, 355–371.

Maillet, D. 1984. Relations des porphyroïdes et schistes de St-Gilles avec les formations siluriennes de Brétignolles-sur-mer (Vendée maritime)—Une tectonique tangentielle par cisaillement ductile pendant l'orogénès acadienne. Thèse 3e cycle Université d'Aix-Marseille.

Marchand, J. 1981. Ecaillage d'un 'mélange tectonique' profond: le complexe cristallophyllien de Champtoceaux (Bretagne méridionale). *C. r. Acad. Sci. Paris* **B293**, 223–228.

Montigny, R. & Allègre, J. C. 1974. A la recherche des océans perdus: les éclogites de Vendée témoins métamorphisés d'une ancienne croûte océanique. *C. r. Acad. Sci. Paris* **D279**, 543–545.

Nicolas, A. & Vialon, P. 1980. Les mécanismes de la déformation ductile. Mem, hors série. *Soc. geol. Fr.* **10**, 127–139.

Quinquis, H., Audren, C., Brun, J. P. & Cobbold, P. R. 1978. Intense progressive shear in Ile de Groix blue schists and compatibility with subduction or obduction. *Nature, Lond.* **273**, 43–45.

Quinquis, H. & Choukroune, P. 1981. Les schistes bleus de l'île de Groix dans la chaîne hercynienne: implications cinématiques. *Bull. Soc. geol. Fr. 7 Sér.* **23, 4**, 409–418.

Ramsay, J. G. 1980a. The crack–seal mechanism of rock deformation. *Nature, Lond.* **284**, 135–139.

Ramsay, J. G. 1980b. Shear zone geometry: a review. *J. Struct. Geol.* **2**, 83–89.

Robin, P. Y. 1979. Theory of metamorphic segregation and related processes. *Geochim. cosmochim. Acta.* **43**, 1587–1600.

Simpson, C. 1983. Strain and shape-fabric variations associated with ductile shear zones. *J. Struct. Geol.* **5**, 61–72.

Simpson, C. & Schmid, S. M. 1983. An evaluation of criteria to deduce the sense of movement in sheared rocks. *Bull. geol. Soc. Am.* **94**, 1281–1288.

Spry, A. 1968. *Metamorphic Textures.* Pergamon, Oxford.

Ters, M. 1970. Découverte d'un gisement de graptolites du Silurien (Wenlock) dans la série de Brétignolles. *C. r. Acad. Sci. Paris* **D271**, 1060–1062.

Ters, M. 1977. Feuille Palluau-île d'Yeu, 2e edn., *Carte Géol. France*, 1:80.000, No. 129.

Ters, M. 1979. Les synclinoriums paléozoiques et le Précambrien sur la façade occidentale du Massif vendéen. Stratigraphie et structure. *Bull. Bur. Rech. géol. min. Fr.* **14**, 293–301.

Tullis, J., Christie, J. M. & Griggs, D. T. 1973. Microstructures and preferred orientations of experimentally deformed quartzites. *Bull. geol. Soc. Am.* **84**, 297–314.
Tullis, J., Snoke, A. W. & Todd, V. R. 1982. Significance and petrogenesis of mylonitic rocks. *Geology* **10**, 227–230.
Tullis, J. & Yund, R. A. 1985. Dynamic recrystallization of feldspar: a mechanism for ductile shear zone formation. *Geology* **13**, 238–241.
Vidal, P. 1980. L'évolution polyorogénique du Massif armoricain: apport de la géochronologie et de la géochimie du strontium: *Mém. Soc. géol. minér. Bretagne* **21**.
Williams, G. D. 1978. Rotation of contemporary folds into the X-direction during overthrust processes in Laksefjord, Finmark. *Tectonophysics* **48**, 29–40.